

A study of the oxidation products of some LiRF_4 phases

H. SAFI, I. R. HARRIS

Department of Physical Metallurgy and Science of Materials, University of Birmingham, Birmingham, UK

B. COCKAYNE, J. G. PLANT

Royal Signals and Radar Research Establishment, Malvern, Worcs, UK

The effects of oxidation in both normal and moist air upon powdered single crystals of the scheelite-type compounds LiYF_4 , LiErF_4 , $\alpha\beta\text{-YLF}$ ($\text{LiY}_{0.434}\text{Er}_{0.5}\text{Tm}_{0.055}\text{Ho}_{0.011}\text{F}_4$) and $\alpha\beta\text{-LuLF}$ ($\text{LiLu}_{0.434}\text{Er}_{0.5}\text{Tm}_{0.055}\text{Ho}_{0.011}\text{F}_4$) have been studied by X-ray powder diffraction and differential thermal analysis. For all the materials the oxidation rate is enhanced in the presence of moisture. The oxidation process results in the formation of rare-earth oxyfluoride phases, LiYF_4 forming yttrium oxyfluoride (with a rhombohedral phase predominating) and LiErF_4 forming erbium oxyfluoride (with a tetragonal phase predominating). The LiYF_4 compound oxidizes more rapidly than LiErF_4 both in normal and moist air. The more complex $\alpha\beta\text{-YLF}$ compound oxidizes to form a mixture containing significant quantities of both the rhombohedral and tetragonal rare-earth oxyfluoride phases. The $\alpha\beta\text{-LuLF}$ compound oxidizes to form the tetragonal rare-earth oxyfluoride phase together with a very small amount of the rhombohedral variety. The melting reactions of oxidized samples are very broad thermal events which are coupled with the presence of a strong LiF/LiRF_4 -type eutectic component. These observations are rationalized in terms of the appearance of excess LiF due to selective oxidation of the trifluoride component.

1. Introduction

Single crystals of certain rare-earth mixed fluorides based on the scheelite-type LiRF_4 (R = rare-earth ion or mixture thereof) compounds can be used as eye-safe solid-state lasers [1, 2]. These crystals are grown using the Czochralski technique from a melt composed of appropriate amounts of the individually zone-refined bars of the LiRF_4 compounds which constitute the complex. The complexes examined here are $\text{Li}(\text{Y}_{0.434}\text{Er}_{0.5}\text{Tm}_{0.055}\text{Ho}_{0.011})\text{F}_4$, known as $\alpha\beta\text{-YLF}$ and $\text{Li}(\text{Lu}_{0.434}\text{Er}_{0.5}\text{Tm}_{0.055}\text{Ho}_{0.011})\text{F}_4$, known as $\alpha\beta\text{-LuLF}$. Translucent and opaque regions which sometimes occur in these otherwise clear single crystals have been shown by X-ray powder diffraction to exhibit lines additional to those characteristic of the tetragonal scheelite structure and these can be attributed to impurity phases. The present work was designed to identify

these phases and thereby help to establish the nature and origin of the impurities in these materials. Mass spectrometric analysis has established that the content of impurities with atomic numbers between 5 and 92 (except for C and O) is low [2]; hence, the most likely impurities are oxygen, water vapour or complexes formed with these species. Thus, X-ray diffraction and differential thermal analysis (DTA) studies have been carried out on material obtained from transparent, translucent and opaque regions of both zone-refined and Czochralski material (a) in its as-grown state, (b) when oxidized in air at 600°C and, (c) when oxidized in moist air at 600°C .

2. Experimental procedure

2.1. Crystalline preparation

A description of the starting materials and the

preparation procedures used in the production of the zone-refined bars and single crystals used here has been given in other publications [2, 3]. Powdered samples were prepared from optically clear and opaque regions of both zone-refined bars of LiYF_4 , LiErF_4 , $\alpha\beta\text{-YLF}$, $\alpha\beta\text{-LuLF}$ and Czochralski crystals of $\alpha\beta\text{-YLF}$ and $\alpha\beta\text{-LuLF}$. Both the bars and crystals are predominantly clear whilst the opaque region is the last portion to crystallize. Occasionally, the bulk of a bar or crystal or the transition region from optically clear to opaque material can be translucent and such material has also been studied. It is known from earlier studies [3, 4] that the translucent and particularly the opaque material contains excess constituents as second phase, that is excess LiF or RF_3 with respect to LiRF_4 . It should be noted however that even the opaque material consists predominantly of the particular LiRF_4 compound.

2.2. Oxidation experiments

Powder samples, prepared by rotary grinding to a particle size of approximately $50\ \mu\text{m}$, were contained in an alumina boat and heated either in normal or moist air at 600°C for up to 20 h.

2.3. X-ray diffraction and differential thermal analysis

After oxidation each sample was examined by (a) X-ray powder diffraction using $\text{CrK}\alpha$ radiation in the standard Debye–Scherrer technique, and (b) differential thermal analysis (DTA) using a Linseis L62 analyser in the manner described previously [3, 4]. For the DTA, special conditions were the use of purified argon to prevent undesirable contamination and a reduction in linear heating rate from 10 to 2°C min^{-1} at thermal events in order to enhance resolution. Unreacted powder samples were also studied as standards.

3. Results and discussion

3.1. X-ray diffraction studies

3.1.1. $\alpha\beta\text{-YLF}$ oxidation

The diffraction patterns of the powder obtained from clear material exhibit diffraction lines characteristic of the tetragonal scheelite structure only. In contrast, corresponding patterns of opaque material and, to a lesser extent, translucent material, exhibit additional very weak low-angle lines which can be attributed to the presence of impurity phases. The d -spacings of these low-angle lines are, 4.99, 4.68, 3.27 and $3.14\ \text{\AA}$.

After the oxidation treatments outlined above, the diffraction patterns show marked changes. The clear material still exhibits strong lines characteristic of the scheelite-type structure but with additional lines. These additional lines are more intense in the diffraction patterns of powders oxidized in moist air. In contrast with the behaviour of the clear material, the diffraction patterns from opaque and translucent material exhibit evidence of a substantial phase change after high-temperature oxidation, particularly in moist air, where the patterns change completely from the original scheelite structure. Typical diffraction patterns are shown in Fig. 1.

A common feature of the diffraction patterns obtained from the oxidized powders is the strengthening of the impurity line at $d = 3.14\ \text{\AA}$, originally observed in unoxidized opaque samples, and the disappearance of the other lines. Fig. 1 shows that this line appears on heating powdered clear material at 600°C in air for only 10 min.

The diffraction patterns indicate that the changes caused by heating in moist and dry air are the same, the effect of the water vapour being to increase the rate at which these changes occur.

3.1.2. LiYF_4 , LiErF_4 , YF_3 , ErF_3 and LiF oxidation studies

In order to elucidate the nature of the changes that occur on oxidizing $\alpha\beta\text{-YLF}$, powders from zone-refined bars of its major constituents, LiYF_4 and LiErF_4 (both clear and opaque material), were reacted under identical conditions to those outlined above. X-ray diffraction studies of these compounds, (see Fig. 2), show that: (a) the LiYF_4 powder is more reactive than the corresponding LiErF_4 powder which could suggest that LiYF_4 is the least stable of these two phases, (b) only the LiErF_4 powder (opaque material) exhibits the $3.14\ \text{\AA}$ impurity line in the as-grown state, (c) powdered material of both phases exhibits extensive reactivity, particularly in moist air conditions, to the extent that the LiYF_4 powder shows none of the original compound lines after annealing in moist air at 600°C for 4 h. However, for LiErF_4 , original compound lines are still visible after an identical treatment, and (d) the diffraction patterns of the oxidized powders of LiYF_4 and LiErF_4 (opaque material) are distinctly different from one another.

Figs 1 and 2 show that the pattern of the oxidized $\alpha\beta\text{-YLF}$ powder (opaque material) is

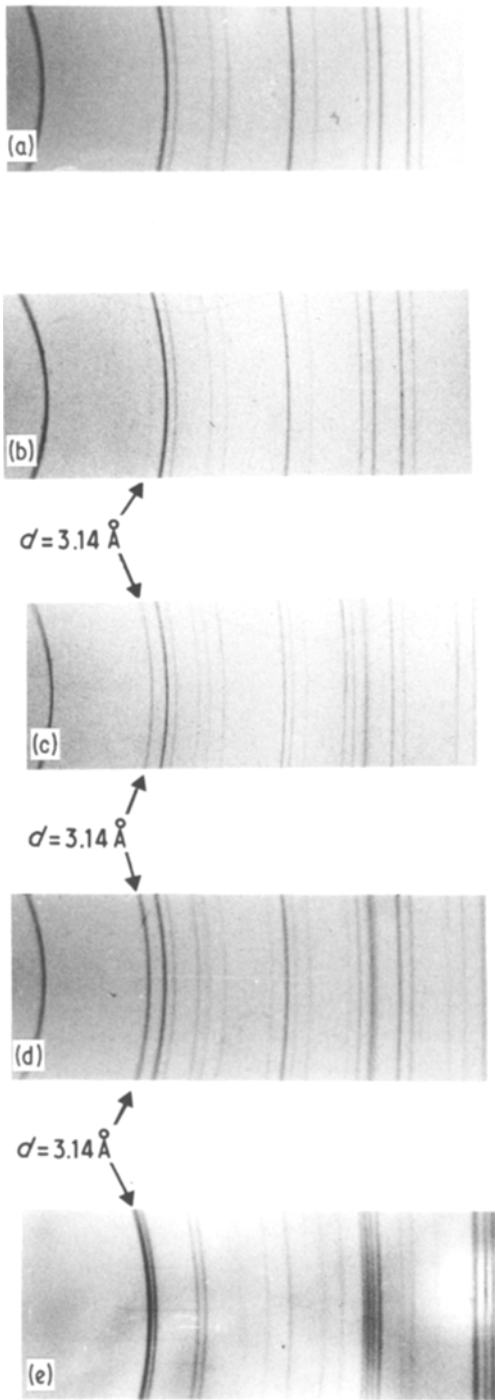


Figure 1 The Debye–Scherrer patterns of oxidized $\alpha\beta$ -YLF. (a) Czochralski $\alpha\beta$ -YLF clear as-received (scheelite-type structure) (b) Czochralski $\alpha\beta$ -YLF clear heated in air for 10 min at 600° C. The impurity line $d = 3.14 \text{ \AA}$ is faintly visible. (c) Czochralski $\alpha\beta$ -YLF clear oxidized in air at 600° C for 4 h. (d) Zone-refined $\alpha\beta$ -YLF opaque oxidized in air at 600° C for 4 h. (e) Zone-refined $\alpha\beta$ -YLF opaque oxidized in moist air for 4 h at 600° C.

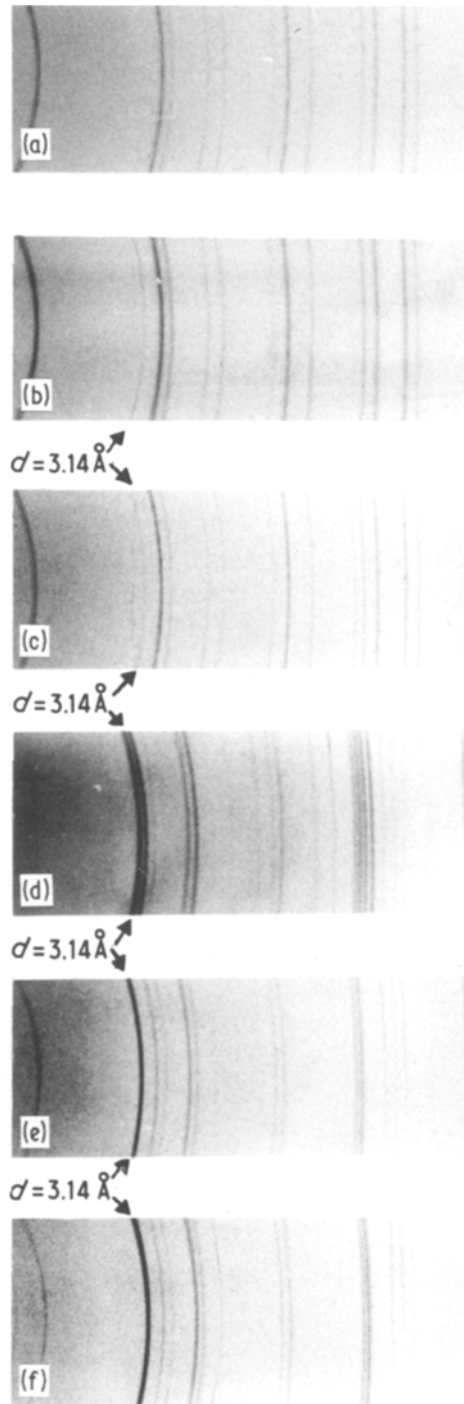


Figure 2 The Debye–Scherrer patterns of oxidized LiYF_4 and LiErF_4 (opaque Czochralski material). (a) LiYF_4 opaque as-received. The impurity line $d = 3.14 \text{ \AA}$ is absent. (b) LiErF_4 opaque as-received. The impurity line $d = 3.14 \text{ \AA}$ is visible. (c) LiYF_4 opaque oxidized in air for 4 h at 600° C. (d) LiYF_4 opaque oxidized in moist air for 4 h at 600° C. (e) LiErF_4 opaque oxidized in air for 4 h at 600° C. (f) LiErF_4 opaque oxidized in moist air for 4 h at 600° C.

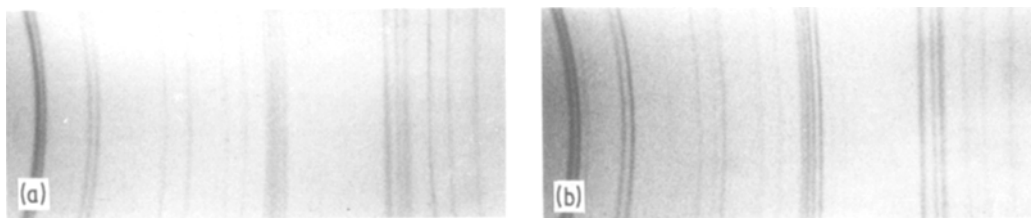


Figure 3 The Debye-Scherrer patterns of (a) oxidized Czoehrski $\alpha\beta$ -YLF (opaque material) in moist air for 4 h at 600°C and (b) the composite pattern of oxidized LiYF_4 and LiErF_4 (opaque materials) under conditions similar to (a).

much more complicated than those of the oxidized LiYF_4 and LiErF_4 powders. If, however, the latter two patterns are superimposed, an excellent match of the line sequence is obtained with the oxidized $\alpha\beta$ -YLF powder (see Fig. 3). Thus, the oxidation process in $\alpha\beta$ -YLF results in the formation of at least two reaction products with the same structures and closely similar d -spacings as oxidized LiYF_4 and LiErF_4 . However, because of the relatively very weak X-ray scattering power of Li atoms compared with rare-earth atoms, these diffraction patterns provide no information on Li-rich phases which might form during oxidation. In consequence, the principal components of the complex compound, namely, LiF , YF_3 and ErF_3 were also heated in moist air for comparison of their reaction products with those of LiYF_4 and LiErF_4 . No change is observed in the diffraction pattern from LiF , even after oxidation at 600°C for 20h; hence, no contribution to the patterns of oxidized scheelites is likely from LiF . The diffraction pattern of oxidized YF_3 is identical to the tetragonal structure of yttrium oxyfluoride plus some weak lines due to the rhombohedral variant of this phase [5, 6]. The pattern of oxidized ErF_3 is identical to the rhombohedral structure of erbium oxyfluoride [5, 6]. Comparison of these

diffraction patterns for oxidized YF_3 and ErF_3 (Fig. 4) with those for oxidized LiYF_4 and LiErF_4 shows conclusively that the oxidation products of the latter two phases are, respectively, yttrium oxyfluoride with the rhombohedral structure and erbium oxyfluoride with the tetragonal structure.

It should be noted that the structures of the oxidation products for the scheelites are the inverse of those for the corresponding fluorides. This apparent difference in behaviour can be rationalized by the work of Niihara and Yajima [6] who showed that a rhombohedral oxyfluoride occurs at the stoichiometric composition, ROF , whereas a tetragonal oxyfluoride occurs at the composition $\text{R}_4\text{O}_3\text{F}_6$ but with a large range of homogeneity. Thus, the inverse behaviour of the trifluorides and scheelites upon oxidation merely reflects the formation of oxyfluorides with different stoichiometries.

For completion, it should be noted that there is no evidence of oxide presence (Y_2O_3 or Er_2O_3) on any of the diffraction patterns of oxidized LiRF_4 or RF_3 materials.

These observations establish that heating $\alpha\beta$ -YLF in air yields reaction products based on the tetragonal and rhombohedral rare-earth oxyfluoride phases, the rare-earth component being a mixture of the constituent rare-earths

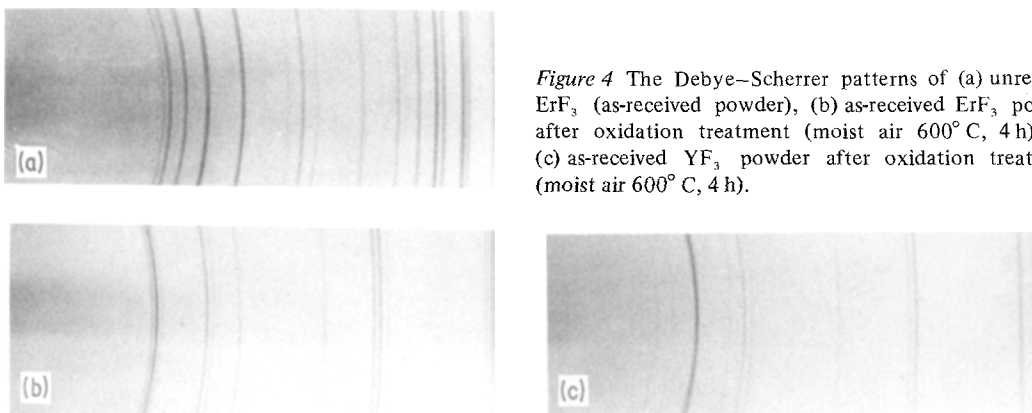


Figure 4 The Debye-Scherrer patterns of (a) unreacted ErF_3 (as-received powder), (b) as-received ErF_3 powder after oxidation treatment (moist air 600°C , 4 h) and (c) as-received YF_3 powder after oxidation treatment (moist air 600°C , 4 h).

(typically $\text{Y}_{0.434}\text{Er}_{0.5}\text{Tm}_{0.055}\text{Ho}_{0.011}$). The co-existence of the two forms of the oxyfluoride phase can be attributed to different stoichiometries of the two variants, as discussed earlier. Dissociation of the compound into individual oxyfluoride phases such as YOF and ErOF is unlikely as this would lead to significant broadening of individual reflections, which is not observed.

3.1.3. $\alpha\beta$ -LuLF oxidation studies

The diffraction pattern of powder obtained from clear $\alpha\beta$ -LuLF crystals exhibited only lines due to the scheelite structure, whereas powder from opaque material exhibited additional weak low-angle lines at similar d -spacings to those observed in the corresponding $\alpha\beta$ -YLF diffraction pattern.

When powdered opaque $\alpha\beta$ -LuLF is oxidized for 4 h at 600°C in moist air, fundamental changes in the X-ray diffraction pattern occur. As in the case of $\alpha\beta$ -YLF, the scheelite lines disappear completely and are replaced by a new set of very well resolved diffraction lines, even at high Bragg angles, as illustrated in Fig. 5. Comparison of this pattern with those described earlier shows almost complete identity with oxidized LiErF_4 powder, the only differences being a small displacement of all lines to lower d -spacings and the presence of some additional, weak, low-angle reflections. This displacement is consistent with the lower mean ionic diameter of the composite R-component ($\text{Lu}_{0.434}\text{Er}_{0.5}\text{Ho}_{0.011}\text{Tm}_{0.055}$) compared with that of erbium. The absence of any phase separation into the individual rare-earth oxyfluorides is indicated by the very well resolved, high-angle reflections. Comparison with erbium oxyfluoride shows that the structure of the predominant phase is tetragonal but as the additional weak low-angle lines correspond with the same sequence of lines exhibited by yttrium oxyfluoride, the presence of a small percentage of the rhombohedral phase is indicated.

The diffraction pattern of an opaque $\alpha\beta$ -LuLF sample heated in air at 600°C and then examined by DTA exhibited only lines due to the rhombohedral structure. This observation is consistent with the arguments based on stoichiometry presented earlier since the stoichiometry and therefore the structure of the rare-earth oxyfluoride phase is likely to depend upon the particular thermal history of the sample. The well resolved diffraction pattern again precludes dissociation into the individual rare-earth oxyfluorides.

3.2. Reaction kinetics

The powdered opaque material was observed to be much more reactive than the corresponding clear material. This could be due to the presence of some oxyfluoride or an excess of one of the components (LiF or RF_3), which would necessarily imply a lower relative stability for the opaque material. For both materials the oxidation process is enhanced by the presence of water vapour. As mentioned earlier, very weak additional lines were observed in the diffraction patterns of as-grown opaque samples of $\alpha\beta$ -YLF and LiErF_4 . Apart from the line with $d = 3.14 \text{ \AA}$, these additional lines disappear on subsequent oxidation at 600°C . Such behaviour could be associated with the formation of a hydroxide phase as an intermediate step in forming the oxyfluoride.

Examination of the reacted powders indicated, as expected, that the oxidation process is surface dominated. This was confirmed by further crushing

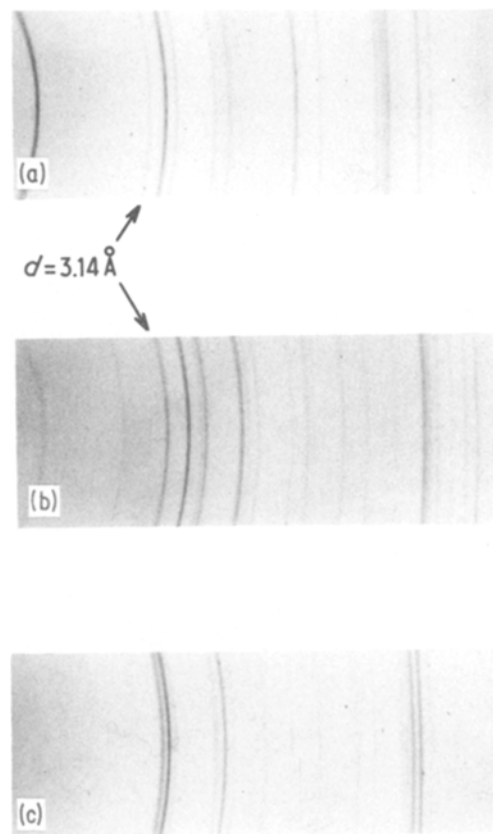


Figure 5 The Debye-Scherrer patterns of (a) unreacted $\alpha\beta$ -LuLF (opaque Czochralski material), (b) oxidized $\alpha\beta$ -LuLF (opaque Czochralski material), 600°C , 4 h and (c) sample from (b) after DTA investigation.

some oxidized $\alpha\beta$ -YLF opaque powdered material, the diffraction pattern of which exhibited strong lines due to the reaction product. The recrushing produced significant enhancement of diffraction lines attributable to the original $\alpha\beta$ -YLF phase.

The changes in intensity of the various diffraction lines on oxidization of the $\alpha\beta$ -YLF powders indicate that the first phase to form (after the formation of a possible intermediate hydroxide) is the tetragonal oxyfluoride which gives rise to the strong reflection with a d -spacing of 3.14 Å. The rhombohedral phase appears at a later stage in the oxidation process, which is entirely consistent with the work of Niihara and Yajima [6] who showed that the tetragonal phase occurs around $R_4O_3F_6$ ($R/O = 1.33$) whereas the rhombohedral phase occurs at ROF ($R/O = 1.0$).

3.3. DTA studies

DTA studies of melting reactions provide constitutional information on the whole of the powder samples, not only the surface. Thus, information obtained from DTA studies on powder oxidized

without recrushing relates mainly to the underlying bulk material and is therefore complementary to that obtained from X-ray diffraction studies. Typical DTA melting profiles obtained in the present work are shown in Fig. 6 with general observations summarized in Table I.

The DTA melting profiles of powder obtained from clear zone-refined bars of $\alpha\beta$ -YLF are sharply defined and similar to those observed previously for this material [3, 4]. Samples from translucent regions exhibit broader melting reactions together with a weak reaction around 700°C, due to the presence of some LiF/LiRF₄ eutectic. The sensitivity of DTA measurements due to the presence of excess LiF was even more evident in powder obtained from opaque regions of the zone-refined bars. In these cases, the melting reactions were very broad and accompanied by a much larger eutectic peak around 700°C.

The melting behaviour of the clear materials was changed substantially by oxidation treatment, the sharp melting profiles being replaced either by a much more diffuse melting reaction at lower

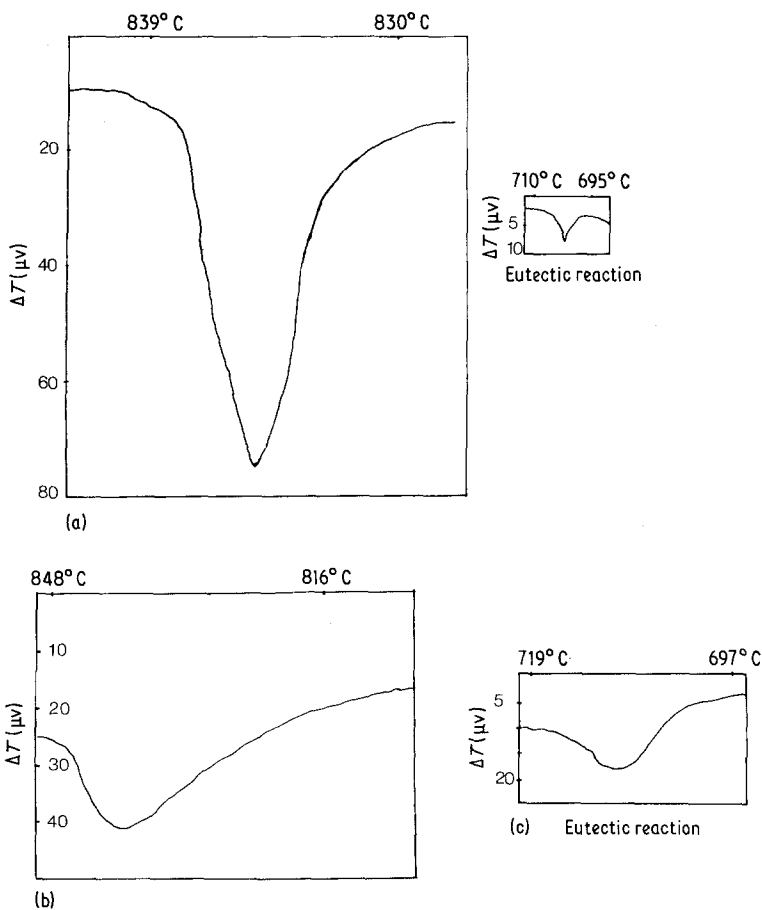


Figure 6 The DTA traces of the melting reactions of (a) an "as-crushed" sample of $\alpha\beta$ -YLF obtained from the translucent region of a Czochralski crystal, (b) and (c) a sample obtained from the same region of the crystal which has been oxidized by heating in moist air at 600°C prior to the DTA study.

TABLE I A summary of some of the DTA results from a variety of $\alpha\beta$ -YLF samples*

Sample description	Pretreatment	Eutectic reaction ($^{\circ}$ C) (10° C min^{-1} heating rate)	Melting reaction ($^{\circ}$ C) (2° C min^{-1} heating rate)	Solidification reaction ($^{\circ}$ C) (2° C min^{-1} heating rate)
ZR - Front - Translucent	None	NO	830-837 (B)	832-827 (S)
ZR - Front - Opaque	None	NO	831-838 (B)	832-827 (DP)
ZR - Rear - Translucent	None	697-714 (WP)	830-837 (B)	827-821 (S)
ZR - Rear - Opaque	None	680-706 (SP)	706-817 (B)	Specimen contaminated
ZR - Rear - Clear	None	NO	829-835 (S)	826-821 (S)
CZ - Centre - Clear	None	NO	840-846 (S)	841-833 (S)
CZ - Rear - Translucent	None	695-707 (WP)	830-839 (S)	Not determined
CZ - Centre - Clear	600 $^{\circ}$ C, normal air	699-710 (SP)	837-853 (B)	Not determined
CZ - Centre - Clear	600 $^{\circ}$ C, moist air	697-710 (SP)	NO	NO
CZ - Rear - Translucent	600 $^{\circ}$ C, normal air	696-710 (SP)	NO	NO
CZ - Rear - Translucent	600 $^{\circ}$ C, moist air	697-719 (SP)	800-840 (VB) (10° C min^{-1} heating rate)	832-813 (B) (10° C min^{-1} heating rate)
			NO	NO
			800-840 (VB) (10° C min^{-1} heating rate)	Not determined

*ZR zone-refined, CZ Czochralski material, NO not observed, B broad melting peak, S sharp melting peak, WP weak peak, SP strong peak, DP double peak.

temperatures or a complete absence of a melting reaction in the temperature range examined. Both these effects were accompanied by the appearance of a strong eutectic reaction at 700°C, a reaction which was totally absent in the original clear material. The presence of a eutectic peak in oxidized material coupled with the lowering of the melting reaction temperature clearly indicates that a LiF/LiRF₄-type eutectic and primary phase mixture is produced by oxidation. These effects are accentuated in oxidized translucent and opaque materials with the very diffuse melting reactions being depressed to even lower temperatures and the eutectic peaks becoming even stronger. Such effects are consistent with these melts being richer in LiF than in the case of oxidized clear material.

The present observations show similarities to those of Abell *et al.* [3, 4], who investigated the melting profiles of some LiY_{1-x}Er_xF₄ compound (0 < x < 1.0) and found that the melting behaviour of these materials was very dependent on the nature of the components (LiF and RF₃) and the melting environment. For example, melting zone-refined material under carefully purified argon produced sharp DTA profiles compared with broad or double peaks at significantly lower temperatures when melting unrefined material in unpurified argon. This behaviour was interpreted in terms of the melt moving to the LiF-rich side of the LiRF₄ composition due to contamination; a possible mechanism suggested for this change was the selective oxidation of the RF₃ component to produce an oxyfluoride [4]. The present work, where much more extreme conditions of contamination have been employed, establishes the authenticity of this mechanism.

4. General discussion and conclusions

The X-ray diffraction studies reported here establish the instability of the LiRF₄ and RF₃ phases and the stability of LiF under the oxidation conditions employed. It is also clear that selective oxidation of LiRF₄ phases produces rare-earth oxyfluorides and hence LiF. Thus, upon oxidation, powdered single phase LiRF₄ changes to a mixture of ROF, R₄O₃F₆ and LiF on the surface of the powder particles with unoxidized LiRF₄ contained within the particle. Upon remelting, as in the DTA studies,

the presence of the excess LiF results in a change from a sharp melting reaction, characteristic of clear material, to a broad melting reaction at a lower temperature together with the appearance of the LiF/LiRF₄ eutectic reaction at around 700°C, due to the mixing of the LiF with the unreacted RLiF₄ phase; the rare-earth oxyfluorides, having high melting points, must remain unmelted. This model is totally consistent with the X-ray diffraction and DTA data on oxidized samples reported here and in previous publications [3, 4].

It is demonstrated that both translucent and opaque LiRF₄ are more readily oxidized than clear material and that the oxidation rates for all the materials are significantly higher in moist air than in normal air conditions.

Oxidation of LiYF₄ yields an yttrium oxyfluoride phase with a rhombohedral structure whereas oxidation of LiErF₄ produces an erbium oxyfluoride phase with a tetragonal structure. This behaviour can be attributed to the formation of oxyfluorides with differing stoichiometries.

Oxidation of αβ-YLF and αβ-LuLF produces a mixture of two rare-earth oxyfluoride structures, the majority phase being tetragonal and the other rhombohedral. There is no evidence of any dissociation into individual rare-earth oxyfluorides and the co-existence of the two structures can be attributed to their different stoichiometries.

Acknowledgements

The work was carried out with the support of the Procurement Executive, Ministry of Defence.

References

1. E. P. CHICKLIS, C. S. NAIMAN, R. C. FOLWEILER, D. R. GABBE, H. P. JENSSEN and A. LINZ, *Appl. Phys. Lett.* **19** (1971) 119.
2. B. COCKAYNE, J. G. PLANT and R. A. CLAY, *J. Cryst. Growth*, to be published.
3. J. S. ABELL, I. R. HARRIS and B. COCKAYNE, *J. Mater. Sci.* **12** (1977) 670.
4. J. S. ABELL, I. R. HARRIS, B. COCKAYNE and J. G. PLANT, *J. Mater. Sci.* **11** (1976) 1807.
5. A. W. MANN and D. J. M. BEVAN, *Acta Cryst.* **B26** (1970) 2129.
6. K. NIIHARA and S. YAJIMA, *Bull. Chem. Soc. Japan* **44** (1971) 643.

Received 30 March and accepted 24 April 1981.